THE JOURNAL OF PHYSICAL CHEMISTRY B

Article

pubs.acs.org/JPCB

Protein-Style Dynamical Transition in a Non-Biological Polymer and a Non-Aqueous Solvent

E. Mamontov,[*,†] V. K. Sharma,[‡,§] J. M. Borreguero,[∥] and M. Tyagi[⊥,#]

[†]Chemical and Engineering Materials Division, Neutron Sciences Directorate, Oak Ridge National Laboratory, Oak Ridge, Tennessee 37831, United States

[‡]Biology and Soft Matter Division, Neutron Sciences Directorate, Oak Ridge National Laboratory, Oak Ridge, Tennessee 37831, United States

[§]Solid State Physics Division, Bhabha Atomic Research Centre, Mumbai 400085, India

[∥]Neutron Data Analysis and Visualization Division, Neutron Sciences Directorate, Oak Ridge National Laboratory, Oak Ridge, Tennessee 37831, United States

[⊥]National Institute of Standards and Technology Center for Neutron Research, Gaithersburg, Maryland 20899, United States

[#]Department of Materials Science and Engineering, University of Maryland, College Park, Maryland 20742, United States

ABSTRACT: Temperature-dependent onset of apparent anharmonicity in the microscopic dynamics of hydrated proteins and other biomolecules has been known as protein dynamical transition for the last quarter of a century. Using neutron scattering and molecular dynamics simulation, techniques most often associated with protein dynamical transition studies, we have investigated the microscopic dynamics of one of the most common polymers, polystyrene, which was exposed to toluene vapor, mimicking the process of protein hydration from water vapor. Polystyrene with adsorbed toluene is an example of a solvent−solute system, which, unlike biopolymers, is anhydrous and lacks hydrogen bonding. Nevertheless, it exhibits the essential traits of the dynamical transition in biomolecules, such as a specific dependence of the microscopic dynamics of both solvent and host on the temperature and the amount of solvent adsorbed. We conclude that the protein dynamical transition is a manifestation of a universal solvent−solute dynamical relationship, which is not specific to either biomolecules as solute, or aqueous media as solvent, or even a particular type of interactions between solvent and solute.

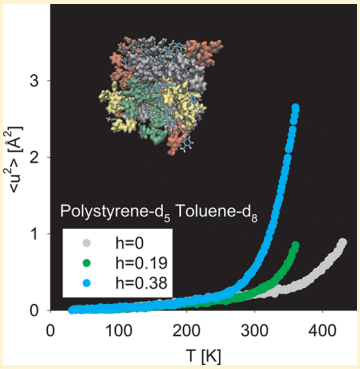

1. INTRODUCTION

Measurements over a broad temperature range are invaluable in studies of microscopic dynamics of proteins and other biomolecules. On warming up from a baseline temperature, often in the range of several Kelvin, where only vibrational degrees of freedom are detected, various relaxation-type processes gradually become visible, eventually coming to dominate the microscopic dynamics of biomolecules at ambient temperatures. The idea of protein dynamical transition has become universally accepted as an attempt to rationalize the principles governing the microscopic dynamics of biomolecules. The dynamical transition manifests itself in the onset of apparent anharmonicity due to activation of the relaxation degrees of freedom, commonly detected in measurements of the temperature dependence of the mean-squared atomic displacements (MSDs). If the dynamical transition temperature is resolution-dependent, it means that the relaxation degrees of freedom actually become activated at lower temperature, and the apparent onset of amharmonicity at the dynamical transition merely reflects the fact that the relaxations have become fast enough to be resolved with the resolution of the measurement.

Even dehydrated proteins exhibit some apparent anharmonicity (e.g., due to relaxation-type dynamics of side chains such as methyl groups), but the main dynamical transition, observed within the 180−240 K temperature range, is strongly hydration-dependent. The defining influence of the aqueous solvent on the picosecond−nanosecond (ps−ns) time scale of biopolymer dynamics has been widely acknowledged,[1,2] even though its exact mechanisms remain debated.[3−7] Incoherent quasielastic neutron scattering (QENS) has become a tool of choice for studying the protein dynamical transition,[8,9] largely due to its ability to measure separately the dynamics of the hydrated host and its hydration water using hydrogenated vs deuterated constituents. The ps−ns accessible time scale and (H/D) sensitivity makes QENS a powerful tool for studying microscopic dynamics of not only biopolymers but polymers in general.[10]

In recent years, some studies have taken a less conventional approach to the problem of solvent−solute microscopic dynamic coupling. One line of studies has established that

Received: January 26, 2016
Revised: February 29, 2016
Published: March 15, 2016

DOI: 10.1021/acs.jpcb.6b00866
J. Phys. Chem. B 2016, 120, 3232−3239

Table 1. Settings for the Equilibration MD Runs

run number	run type	T_i (K)	T_f (K)	Langevin damping period (fs)	P_i (atm)	P_f (atm)	pressure damping period (ps)	simulation time (ns)	time step (fs)
1	compress	10	10	10	0	100	100	0.2	0.1
2	compress	10	10	10	10	10	100	0.5	0.1
3	compress	10	10	10	1	10	10	1	0.1
4	compress	10	10	10	10	10	10	0.1	1
5	compress	10	10	10	10	10	100	2	1
6	compress	10	10	10	10	1	100	5	1
7	heating	10	450	20000	1	1	100	4.5	1

the dynamical transition is essentially independent of protein structure[11,12] and observed even in denatured proteins[13] and amino acid mixtures.[14] Another line of studies has revealed[15−17] that water hydrating even "rigid" inorganic compounds exhibits the same characteristic temperature and hydration level dependence of MSD and relaxation time as displayed by water hydrating proteins and other biomolecules.[18,19] These findings suggest that hydration water may be solely responsible for the main characteristic features of the dynamical transition, while in turn experiencing the influence of the host, e.g., through acquiring host-specific hydration level and assuming the relaxation dynamics specific to this particular hydration level.

We hypothesize that the dynamical transition in the hydration water and, by extension, the protein host is merely a manifestation of a universal solvent−solute relationship independent of composition, chemical bonding, and physical interactions in the solvent−solute system. To test this hypothesis, we follow a protocol commonly adopted in studies of protein powders hydrated in a controlled manner from water vapors but use a simple nonbiological polymer, polystyrene (PS), exposed to vapors of toluene. Unlike in hydrated biopolymers, there is no hydrogen bonding in the PS−toluene system, which is instead dominated by dispersion forces and by $\pi-\pi$ interactions between aromatic rings. Nevertheless, this nonbiological polymer and nonaqueous solvent reproduce the essential features of the protein dynamical transition, including its dependence on the amount of adsorbed solvent and the strong coupling of the host to the translational dynamics of the adsorbed solvent.

2. EXPERIMENT AND SIMULATION

Samples. Because of the dominant incoherent neutron scattering cross section of hydrogen compared to other elements, including deuterium, we use PS-d_3 (deuterated backbone) and PS-d_5 (deuterated aromatic ring side groups) exposed to fully deuterated toluene-d_8 in order to emphasize the scattering signal from the PS side groups and the PS backbone, respectively. Likewise, we use fully deuterated PS-d_8 exposed to methyl-deuterated toluene-d_3 to probe the dynamics of the toluene solvent with the emphasis on its aromatic rings, as opposed to the methyl group.

Fully deuterated toluene ($C_6D_5CD_3$, toluene-d_8) and partially deuterated toluene ($C_6H_5CD_3$, toluene-d_3) were purchased from Sigma-Aldrich. Fully and partially deuterated atactic polymers, ($-C_6D_5CD_2CD-$, PS-d_8, M_n = 15,800), ($-C_6H_5CD_2CD-$, PS-d_3, M_n = 15,000), and ($-C_6D_5CH_2CH-$, PS-d_5, M_n = 4,500), were purchased from Polymer Source Inc. The as received polymers have been separately vacuum-annealed at 363 K for 2 days, resulting in a maximum weight loss of 0.6%. The annealing process removes the residual volatile contaminants from the polymer samples and is conceptually equivalent to protein sample lyophilization prior to controlled hydration. A control annealed sample was stored on a benchtop in an open dish for about 72 h, without any significant weight uptake, as expected from hydrophobic interactions between polystyrene and atmospheric water. Three of the annealed samples, one of each H−D composition, were then sealed with indium wire in annular aluminum sample holders and subsequently used as h = 0 samples in the neutron scattering experiments. Here h is the solvent uptake, in grams per gram of sample, using the notation commonly employed for hydrated proteins. Six of the annealed samples, two of each H−D composition, were then placed in enclosed chambers that also contained open dishes of either toluene-d_8 or toluene-d_3. The continuously increasing uptake of toluene by polystyrene from the vapors was then monitored for about 24 h, and upon reaching the target uptake, the samples were removed from the chambers and sealed with indium wire in annular aluminum sample holders. Altogether we prepared the following nine samples for neutron scattering experiments: polystyrene-d_3−toluene-d_8 at h = 0, 0.19, and 0.39, polystyrene-d_5−toluene-d_8 at h = 0, 0.19, and 0.38, and polystyrene-d_8−toluene-d_3 at h = 0, 0.20, and 0.44. The mass of polystyrene samples prior to their exposure to toluene vapor was controlled in order to minimize the effects of multiple scattering in neutron scattering experiments, and varied between 0.33 and 0.47 g among the nine samples.

Neutron Scattering Experiment. Measurements of the nine samples were carried out using the High Flux Neutron Backscattering Spectrometer (HFBS)[20] at the NIST Center for Neutron Research (NCNR), Gaithersburg, MD. A reactor-based backscattering spectrometer such as HFBS (1 μeV energy resolution, FHWM) is an optimal choice for collecting the energy-resolved elastic scattering that can be used to extract the MSD temperature dependence averaged over the hydrogen-bearing species in the sample. The elastic intensity temperature scan measurements have been carried out with the Doppler monochromator at rest in the course of a heating cycle from the baseline temperature of 30 K at a ramp rate of 0.6 K/min with a data point recorded every 2.5 min. The atomic MSD was obtained from the elastic intensities using a Gaussian approximation, $I_{elastic}(Q, T) = I_{elastic}(Q, T_0) \exp(-Q^2\langle u^2(T)\rangle/3)$, with a baseline temperature of T_0 = 30 K and 0.36 Å^{-1} < Q < 1.51 Å^{-1}. Besides, the elastic scattering intensities have been analyzed separately, without calculating the MSD. One of the samples, polystyrene-d_8−toluene-d_3 at h = 0.44, was subsequently measured using the backscattering spectrometer BASIS[21] at the Spallation Neutron Source (SNS), Oak Ridge National Laboratory (ORNL). This spectrometer had an energy resolution of 3.4 μeV FHWM) and a range of accessible

DOI: 10.1021/acs.jpcb.6b00866
J. Phys. Chem. B 2016, 120, 3232−3239

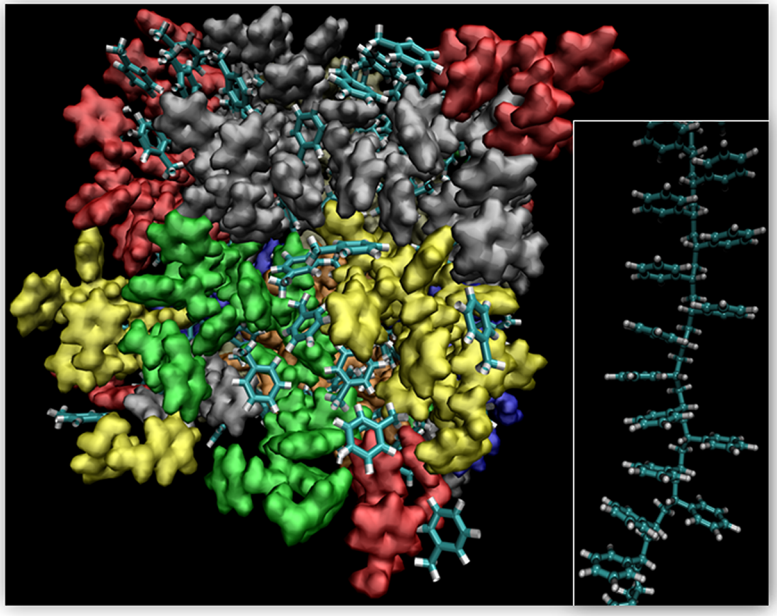

Figure 1. Fully equilibrated MD simulation structure of the styrene−toluene system at h = 0.44 (grams of toluene per gram of styrene), corresponding to one toluene molecule per two styrene monomers. There are eight chains of styrene (colored). The toluene molecules are drawn as sticks. Inset: a fragment of a polystyrene chain drawn as sticks.

energy transfers of ±100 μeV. When not visible in the figures, the error bars are within the size of the symbols.

Molecular Dynamics Simulation. Using the polymer builder tool of Biovia Materials Studio[22] (BMS), we arranged eight atactic polystyrene chains, each 32 monomers long, in a cubic grid with a cell size of 10 nm. This initial configuration was minimized for 400 steps with the BMS module Forcite and the CVFF[23] force field. Using the BMS module "Amorphous Cell", we randomly inserted 128 toluene molecules in the system for a ratio of two styrene monomers per toluene molecule. A second minimization with the previous settings was carried out in this styrene plus toluene system. The final system consists of a gas of polystyrene chains and toluene molecules that is subsequently equilibrated to a target temperature of 450 K and a pressure of 1 atm. To attain equilibration, we first export the minimized system in a format suitable for simulations with the LAMMPS[24] package and the CVFF force field. The initial equilibration protocol consists of a series of compression runs at a constant T = 10 K followed by a slow heating of the system to a target temperature of 450 K at a constant pressure of P = 1 atm (see Table 1).

Once equilibration is achieved at 450 K, a 5 ns run in the NPT ensemble (450 K, 1 atm) is performed. The end conformation of this run is taken as the initial conformation for two runs: (1) a production run of 100 ns at the same temperature of 450 K and (2) an equilibration run of 5 ns at a slightly colder temperature of 440 K. We repeat this protocol, each time collecting a production run at temperature T and an equilibration run at $T' = T - 10$ K, until we reached the lowest simulated temperature (80 K).

In order to make a straightforward comparison between simulation and experiment results, we reproduce the experimental methodology. First, the intermediate neutron self-incoherent scattering function $I(Q, t)$ is calculated with the Sassena[25] package, which is then followed by Fourier transform to obtain $S(Q, E)$ with the SassenaFFT algorithm of the Mantid[26] framework. Convolution with a model function describing the resolution function of the HFBS instrument (a Gaussian centered at E = 0 with FWHM = 0.8 μeV) is carried out, followed by integration in the [−FHWM, FHWM] energy range to finally obtain the elastic signal IESF. The resulting IESF(Q) is fitted to the same Gaussian decay model as in the experiment in order to derive the MSD value. Different hydrogen atoms are considered when comparing to different experimental samples. For instance, only hydrogen atoms in the rings of the toluene molecules were taken into account in the IESF calculation when comparing to the PS-d_8−toluene-d_3 sample.

Trajectories for the center of mass (CoM) of each styrene ring, each styrene backbone, and each toluene ring are generated with the pyTraj[27,28] library. The CoM trajectories are treated in the same way as the atomic trajectories for the purposes of deriving $\langle u_{com}^2 \rangle$ values.

3. RESULTS AND DISCUSSION

The molecular dynamics (MD) simulation snapshot of the PS−toluene system is presented in Figure 1, exhibiting similarity to numerous pictures of hydrated biopolymers available in the literature. However, particularly striking similarity to protein data available from numerous publications is exhibited by Figure 2. The "dry" PS shows essentially harmonic behavior as a function of temperature up to its glass transition of ca. 370 K. The PS with toluene solvent shows apparent temperature-dependent anharmonicity, with a larger increase in MSD and earlier onset of apparent anharmonicity for the higher solvent uptake compared to the lower solvent uptake. The temperature dependence of MSD of PS with variable toluene adsorption shown in Figure 2 looks very similar to that of biopolymers, except for the particular temperature range of the dynamical transition. Besides, we have deliberately heated up the "dry" PS sample above its glass transition temperature of ca. 370 K, leading to the eventual increase in the MSD, even though it

DOI: 10.1021/acs.jpcb.6b00866
J. Phys. Chem. B 2016, 120, 3232−3239

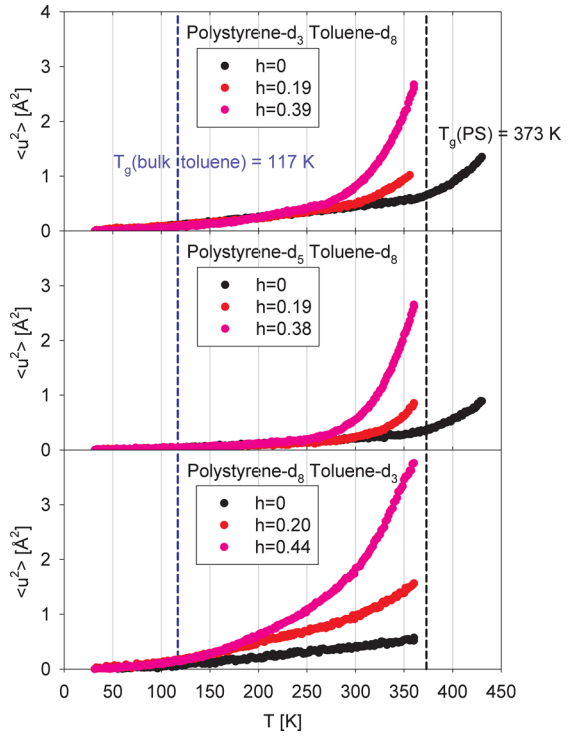

Figure 2. Mean-squared displacements obtained from the temperature dependence of the energy-resolved elastic scattering intensities measured on warming up from the baseline temperature. The glass transition temperatures of polystyrene and bulk toluene are marked by vertical dashed lines.

would correspond to heat denaturation of biomolecules, which is not commonly done in experiments. Also presented in Figure 2 is the glass transition temperature for polystyrene and toluene in bulk form.

The temperature dependence of MSD presented in Figure 2 may enjoy widespread recognition by the biophysics community. It convincingly demonstrates that the dynamical transition in polystyrene is solvent-driven and depends on the amount of solvent in the same manner as the dynamical transition in hydrated proteins. However, strictly speaking, despite its widespread use in the literature, the derivation of the $\langle u^2(T)\rangle$ from the elastic intensities using a Gaussian approximation is no longer valid when relaxation degrees of freedom become activated. For this reason, direct analysis of elastic scattering intensities[29] may be preferred. Since we could not vary the energy resolution of the backscattering spectrometer, the temperature dependence of the elastic intensities at a fixed energy resolution ($\tau_{res} \approx 1500$ ps) needs to be analyzed.

Because of the anticipated complexity of the intermediate relaxation function, $I(Q, t)$, for the system studied, it was approximated by a stretched exponential (Kohlrausch) function

$$I(Q, t) = (1 - \mathrm{EISF}(Q)) \exp(-t/\tau_c(T))^{\beta} + \mathrm{EISF}(Q) \quad (1)$$

where $\mathrm{EISF}(Q)$ is the temperature-independent elastic scattering fraction and $\tau_c(T)$ is the temperature-dependent relaxation time. Following ref 29, we use the δ-resolution function approximation, where the difference between the total elastic scattering fraction and the elastic scattering intensity vanishes, and the measured elastic scattering intensity, $S_R(Q, E = 0)$, is related to the $I(Q, t)$ evaluated at $t = \tau_{res}$:

$$S_R(Q, E = 0) = \frac{1}{\pi} I(Q, t = \tau_{res}) \quad (2)$$

In order to fit the temperature dependence of $S_R(Q, E = 0)$, we make an assumption of the Arrhenius-type relaxation time, $\tau_c(T) = \tau_0 \exp(E_a/RT)$, and the linear temperature dependence of the vibrational displacements of the Debye–Waller factor, which is thus assumed to modulate the experimentally measured $S_R(Q, E = 0)$ proportionally to $\exp(-\alpha T)$. If the energy resolution cannot be varied, which is usually the case in backscattering experiments, there is degeneracy between the stretch parameter, β, and the prefactor of Arrhenius relaxation time, τ_0. Fortunately, at the temperature that manifests the dynamical transition, when $\tau_c(T) = \tau_{res}$, the elastic intensity decays to $(1/e)$ of its initial value, regardless of the stretch parameter, β.[29] Thus, the activation energy, E_a, can be determined reliably, even if the prefactor, τ_0, cannot. Two of the data sets shown in Figure 2 exhibit sufficiently large intensity decay at the highest measured temperature, which makes them suitable for this kind of analysis, as presented in Figure 3.

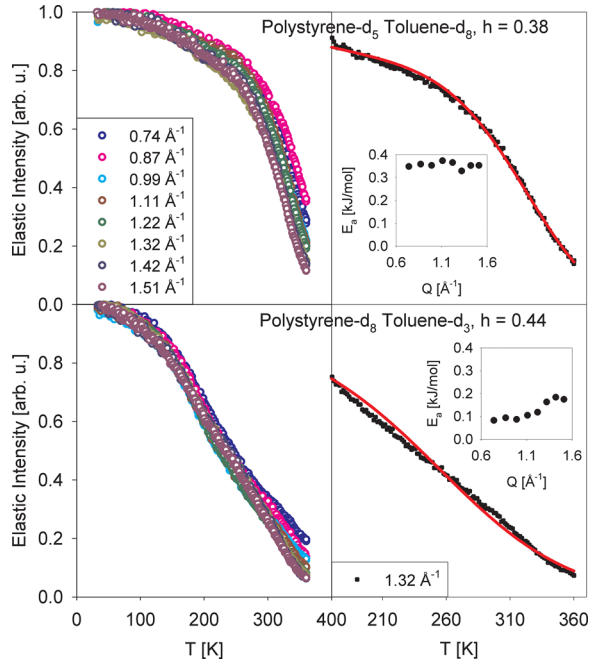

Figure 3. Left panels: Q-dependence of elastic scattering intensities dominated by the solvent (PS-d_8, toluene-d_3) and the polymer matrix (PS-d_5, toluene-d_8). Right panels: analysis of elastic scattering intensities presented at a selected Q value of 1.32 Å^{-1}. Symbols: data. Solid lines: fits with eqs 1 and 2 as described in the text. Insets show the Q-dependence of the activation energy for the relaxations.

Observation of the Q-dependence of elastic intensities suggests that toluene solvent may exhibit more than one relaxation process, whereas polystyrene exhibits only one relaxation, correlated with the higher-temperature relaxation in toluene. This observation is corroborated by the analysis using eqs 1 and 2 as described above. The Kohlrausch relaxation function adequately describes the elastic intensity from polystyrene, yielding a Q-independent activation energy of $E_a \approx 0.35$ kJ/mol, as expected from a localized process. On the other hand, a single Kohlrausch function proves less than adequate for description of the elastic intensity from

DOI: 10.1021/acs.jpcb.6b00866
J. Phys. Chem. B 2016, 120, 3232−3239

polystyrene, suggesting the presence of more than one relaxation process. This is clearly seen in Figure 3 at a selected Q value, and such inadequacy of a single relaxation description, compared to a goof fit for polystyrene data, is observed at all other Q values. The activation energy obtained for toluene is somewhat lower compared to that for polystyrene, and is somewhat Q-dependent, as expected for a solvent with larger molecular displacements, which may be of partially translational origin. As we discuss below, additional experiments and simulation indeed demonstrate the complex character of the toluene solvent dynamics.

Even though we are unaware of prior neutron scattering experiments specifically targeting microscopic dynamics in polymer powders with different levels of solvent uptake, some interesting conclusions may be inferred from the existing literature on neutron scattering studies of PS. Several papers by Kanaya et al. have described the "fast process" in PS with the onset temperature similar to what we observe in the current work, although it is not clear whether the solvent, apparently introduced in the PS samples unintentionally, was toluene or methanol.[30,31] Even though PS phenyl rings were implicated in the detected relaxation dynamics, their full flips have been ruled out as a possible origin of this relaxation process.[31] This prominent relaxation process, which we believe might have been the same as the relaxation observed in the current work, was likely solvent-driven, because similar measurements of the solvent-free PS indicated only very weak relaxation dynamics below the glass transition temperature.[32] This is in agreement with our data in Figure 2 for $h = 0$ samples and numerous studies of solvent-free (dry) proteins that exhibit measurable but weak dynamics in the dry state. It is also possible that the "fast process" dynamics reported for PS films[33] could have been affected by the solvent or lack thereof in the films and control samples, even though the validity of comparison of microscopic relaxation dynamics between films and powder samples could be questioned.

As evidenced by the bottom panel in Figure 2, the toluene solvent itself exhibits a dynamical transition, similar to that demonstrated by hydration water,[16] with the same solvent-level dependence, though shifted in temperature. Quasielastic neutron scattering data for the high solvent level sample, $h = 0.44$, are shown in Figure 4. These spectra were collected from PS-d_8–toluene-d_3 to probe the dynamics of toluene, predominantly its aromatic rings. For clarity, only the lowest- and highest-Q data are shown. The corresponding dynamic susceptibilities presented in the insets show complex, highly heterogeneous microscopic dynamics, as evidenced by the absence of maxima in the susceptibility spectra, which defies the standard data fitting approach that relies on susceptibility maxima to extract the characteristic relaxation times. The complex character of the toluene solvent relaxations corroborates our earlier discussion of elastic intensity temperature dependence demonstrating inadequacy of a single relaxation component (even stretched) for description of toluene. However, from model-independent observation of data in Figure 4, we conclude that the Q-dependence of the scattering spectra changes qualitatively somewhere between 257 and 297 K, as evidenced by the crossing of the low-Q and high-Q spectra in Figure 4 at high, but not low, temperatures. Below 257 K, the low-Q and high-Q signal wings exhibit a similar width, though the wing intensity is higher at high Q. Above 257 K, the high-Q spectra are broader than the low-Q spectra, leading to spectra crossing, as corroborated by crossing in the

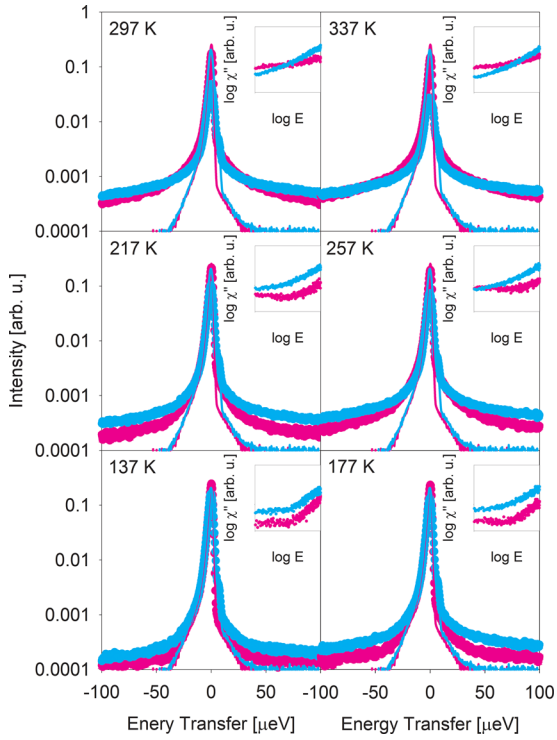

Figure 4. Temperature dependence of the scattering intensity from PS-d_8-toluene-d_3, $h = 0.44$, measured at $Q = 0.5$ Å^{-1} (pink symbols) and $Q = 1.7$ Å^{-1} (cyan symbols). For comparison, the spectra measured at 10 K are shown with solid lines of the same colors. Insets: log–log plots of the scattering intensities converted to dynamic susceptibilities, $\chi''(E) = I(Q, E)/n_b(E)$, where $n_b(E)$ is the thermal Bose factor.

susceptibility plots shown in the insets. Together with the Q-dependent signal intensity, the Q-independent signal width at low temperatures is indicative of the localized diffusion.[34] On the other hand, the Q-dependent signal width at high temperatures indicates long-range translational diffusion.[34] Thus, despite the onset of apparent anharmonicity evident in the bottom panel of Figure 2 already at a low temperature (comparable with the glass-transition temperature of bulk toluene of 117 K), the diffusion of the adsorbed toluene does not become translational until the temperature reaches the 257–297 K range. This solvent behavior is reminiscent of hydration water in an inorganic system, which does not become translationally mobile until 240–250 K, despite starting to exhibit localized diffusion at much lower temperatures.[1] Besides, this suggests that only the high-temperature, but not the low-temperature, relaxation process in toluene visible in the elastic intensity in Figure 3 above ca. 300 K is associated with pronounced translational mobility.

MD simulations allow separation of the atomic mean-squared displacements into the center-of-mass (com) and internal (int) contributions, $\langle u^2 \rangle = \langle u_{com}{}^2 \rangle + \langle u_{int}{}^2 \rangle$, for the toluene molecules and the styrene monomers. This enables assessment of their relative importance through different temperature ranges. The results of such analysis are presented in Figure 5 for the same solvent-level sample of $h = 0.44$. Expectedly, the relative contribution of $\langle u_{com}{}^2 \rangle$ is highest for the backbone dynamics (solid blue line), represented in the experiments by PS-d_5–toluene-d_8 samples. Toluene dynamics, represented in the experiments by PS-d_8–toluene-d_3 samples, expectedly shows the lowest relative contribution of $\langle u_{com}{}^2 \rangle$

DOI: 10.1021/acs.jpcb.6b00866
J. Phys. Chem. B 2016, 120, 3232–3239

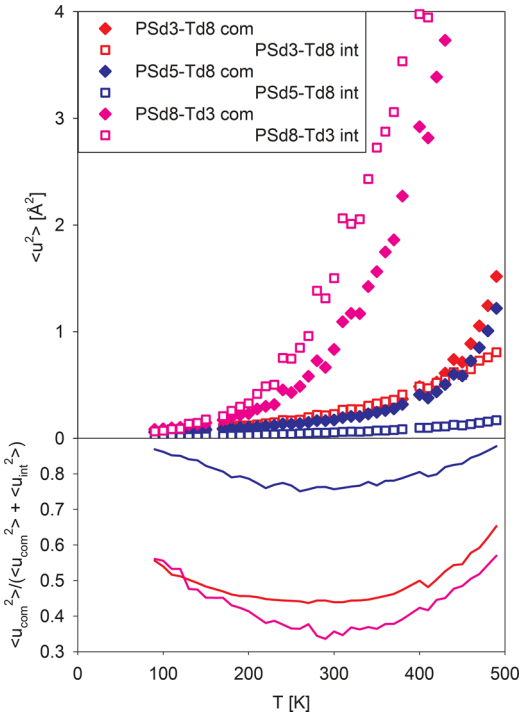

Figure 5. MD simulation results showing the temperature dependence of the mean-squared displacement for polystyrene−toluene at h = 0.44, which corresponds to one toluene molecule per two styrene monomers. Top panel (symbols): center-of-mass (com) and internal (int) displacements, which contribute to the total displacement as $\langle u^2 \rangle = \langle u_{com}^2 \rangle + \langle u_{int}^2 \rangle$. Bottom panel (lines): relative contribution of the center-of-mass displacement, $\langle u_{com}^2 \rangle / \langle u^2 \rangle$.

(solid pink line). The dynamics of PS aromatic rings, represented in the experiments by PS-d_3−toluene-d_8 samples, shows the intermediate relative contribution of the $\langle u_{com}^2 \rangle$ (solid red line), which is nevertheless much closer to the behavior of the toluene solvent (solid pink line) than the backbone (solid blue line). Importantly, the minimum of $\langle u_{com}^2 \rangle / \langle u^2 \rangle$, which immediately precedes the onset of long-range translational diffusion of toluene, is just below 300 K (solid pink line in the bottom panel in Figure 5), corroborating the experimental observations presented in Figure 4 that indicate onset of toluene translational diffusion between 257 and 297 K. The $\langle u_{com}^2 \rangle / \langle u^2 \rangle$ temperature dependence for both the PS side groups and PS backbone reproduces that of toluene, showing the minimum just below 300 K. Analogously, the onset of translational mobility in protein hydration water has been shown to trigger the relaxations in the hydrated protein.[35] Both protein side groups and backbone have been shown to take part in such hydration water-linked relaxations.[36]

4. CONCLUSION

On the basis of the present results with toluene solvent and analogous data previously collected in numerous experiments using hydration water, we summarize the universal traits of the solvent−solute dynamic coupling that gives rise to the "dynamical transition" in powder samples, irrespective of the nature of the solvent and solute, as follows.

1. The "dynamical transition", usually identified as the onset of apparent anharmonicity in the MSD temperature dependence, is intrinsic to any solvent bound to the host surface, irrespective of the host. The amplitude of solvent MSD increases with the amount of solvent on the host surface.
2. A "soft" host is dynamically coupled to its solvent, irrespective of the bonding and physical interactions between the host and solvent. More specifically, the host responds strongly to the onset of the translational dynamics in the solvent. The amplitude of host MSD increases with the amount of solvent on the host surface, just as for the solvent itself.

The difference between "soft" and "hard" hosts (such as oxides or carbon-based materials in contact with a solvent) is that the latter do not exhibit relaxation degrees of freedom. The "soft" hosts, on the other hand, are generally capable of exhibiting relaxations, which can be enhanced or modified by the solvent and can involve, in principle, both segmental motions and the main structural relaxation related to the glass transition. In practice, the pico-to-nanosecond time scale relaxations, accessible in neutron scattering experiments, usually involve segmental or side group relaxation rather than main structural relaxation.[2] For instance, it has been suggested[2] that the main structural relaxation related to glass transition in proteins is represented by the microsecond backbone relaxation process, whereas the relaxation involved in the solvent-driven "dynamical transition" is a secondary process. This scenario agrees with our observation (see Figure 2) that the "dynamical transition" in the solvent and its "soft" host is found above the glass transition temperature of the solvent and below the glass transition temperature of the host.

In view of these findings, the "dynamical transition" in protein (and biomolecules in general) powder samples is merely a manifestation of a universal solvent−solute dynamical relationship, driven by hydration water, but actually not specific to either the biomolecules as solute or even water as solvent.

What are the implications of our findings for studying the microscopic dynamics of biomolecules? In studies of hydrated biomolecules as powders, measurement results are strongly dependent on the variations in the hydration level, negatively affecting reproducibility of the so obtained numerical parameters. This is because any change in the hydration level alters the dynamics of the hydration water and, consequently, the host. On the other hand, there is no hydration level dependence in native environments (solutions), unlike in hydrated powders. Despite methodological difficulties with experiments in native environments over a broad temperature range (prominence of global rotational and translational molecular dynamics and buffer freezing, both of which are absent in hydrated powder samples), the use of solutions is much preferred to the use of hydrated powders, unless one's goal is to investigate merely a rather generic physical−chemical phenomenon of hydration-level dependence of the solvent dynamics, which is not specific to biomolecules.

AUTHOR INFORMATION

Corresponding Author

*E-mail: mamontove@ornl.gov.

Notes

The authors declare no competing financial interest.

ACKNOWLEDGMENTS

The neutron scattering experiments on HFBS at NCNR were supported in part by the National Science Foundation under Agreement No. DMR-1508249. The neutron scattering experi-

DOI: 10.1021/acs.jpcb.6b00866
J. Phys. Chem. B 2016, 120, 3232−3239

ments on BASIS at SNS were supported by the Scientific User Facilities Division, Office of Basic Energy Sciences, U.S. Department of Energy. J.M.B. is supported by the Center for Accelerating Materials Modeling (CAMM) funded by the U.S. Department of Energy, Basic Energy Sciences, Material Sciences and Engineering Division under FWP-3ERKCSNL. This manuscript has been authored by UT-Battelle, LLC under Contract No. DE-AC05-00OR22725 with the U.S. Department of Energy. The United States Government retains and the publisher, by accepting the article for publication, acknowledges that the United States Government retains a nonexclusive, paid-up, irrevocable, worldwide license to publish or reproduce the published form of this manuscript, or allow others to do so, for United States Government purposes. The Department of Energy will provide public access to these results of federally sponsored research in accordance with the DOE Public Access Plan (http://energy.gov/downloads/doe-public-access-plan). Certain commercial material suppliers are identified in this paper to foster understanding. Such identification does not imply recommendation or endorsement by the National Institute of Standards and Technology, nor does it imply that the materials or equipment identified are necessarily the best available for the purpose. The authors declare no competing financial interests.

REFERENCES

(1) Mamontov, E.; Chu, X. Water-Protein Dynamic Coupling and New Opportunities for Probing It at Low to Physiological Temperatures in Aqueous Solutions. *Phys. Chem. Chem. Phys.* **2012**, *14*, 11573−11588.

(2) Khodadadi, S.; Sokolov, A. P. Protein Dynamics: From Rattling in a Cage to Structural Relaxation. *Soft Matter* **2015**, *11*, 4984−4998.

(3) Fenimore, P. W.; Frauenfelder, H.; McMahon, B. H.; Parak, F. G. Slaving: Solvent Fluctuations Dominate Protein Dynamics and Functions. *Proc. Natl. Acad. Sci. U. S. A.* **2002**, *99*, 16047−16051.

(4) Fenimore, P. W.; Frauenfelder, H.; McMahon, B. H.; Young, R. D. Bulk-Solvent and Hydration-Shell Fluctuations, Similar to α- and β-Fluctuations in Glasses, Control Protein Motions and Functions. *Proc. Natl. Acad. Sci. U. S. A.* **2004**, *101*, 14408−14413.

(5) Frauenfelder, H.; Chen, G.; Berendzen, J.; Fenimore, P. W.; Jansson, H.; McMahon, B. H.; Stroe, I. R.; Swenson, J.; Young, R. D. A Unified Model of Protein Dynamics. *Proc. Natl. Acad. Sci. U. S. A.* **2009**, *106*, 5129−5134.

(6) Doster, W.; Settles, M. Protein-Water Displacements Distributions. *Biochim. Biophys. Acta, Proteins Proteomics* **2005**, *1749*, 173−186.

(7) Khodadadi, S.; Roh, J. H.; Kisliuk, A.; Mamontov, E.; Tyagi, M.; Woodson, S. A.; Briber, R. M.; Sokolov, A. P. Dynamics of Biological Macromolecules: Not a Simple Slaving by Hydration Water. *Biophys. J.* **2010**, *98*, 1321−1326.

(8) Doster, W.; Cusack, S.; Petry, W. Dynamical Transition of Myoglobin Revealed By Inelastic Neutron Scattering. *Nature (London, U. K.)* **1989**, *337*, 754−756.

(9) Doster, W. The Two-Step Scenario of the Protein Dynamical Transition. *J. Non-Cryst. Solids* **2011**, *357*, 622−628.

(10) Colmenero, J.; Arbe, A. Recent Progress on Polymer Dynamics by Neutron Scattering: From Simple Polymers to Complex Materials. *J. Polym. Sci., Part B: Polym. Phys.* **2013**, *51*, 87−113.

(11) Sacquin-Mora, S.; Sebban, P.; Derrien, V.; Frick, B.; Lavery, R.; Alba-Simionesco, C. Probing the Flexibility of the Bacterial Reaction Center: The Wild-Type Protein is More Rigid than Two Site-Specific Mutants. *Biochemistry* **2007**, *46*, 14960−14968.

(12) He, Y.; Ku, P. I.; Knab, J. R.; Chen, J. Y.; Markelz, A. G. Protein Dynamical Transition Does Not Require Protein Structure. *Phys. Rev. Lett.* **2008**, *101*, 178103.

(13) Mamontov, E.; O'Neill, H.; Zhang, Q. Mean-Squared Atomic Displacements in Hydrated Lysozyme, Native and Denatured. *J. Biol. Phys.* **2010**, *36*, 291−297.

(14) Schiro, G.; Caronna, C.; Natali, F.; Koza, M. M.; Cupane, A. The "Protein Dynamical Transition" Does Not Require the Protein Polypeptide Chain. *J. Phys. Chem. Lett.* **2011**, *2*, 2275−2279.

(15) Mamontov, E.; Vlcek, L.; Wesolowski, D. J.; Cummings, P. T.; Rosenqvist, J.; Wang, W.; Cole, D. R.; Anovitz, L. M.; Gasparovic, G. Suppression of the Dynamic Transition in Surface Water at Low Hydration Levels: A Study of Water on Rutile. *Phys. Rev. E* **2009**, *79*, 051504.

(16) Mamontov, E.; O'Neill, H.; Zhang, Q.; Wang, W.; Wesolowski, D. J. Common Features in the Microscopic Dynamics of Hydration Water on Organic and Inorganic Surfaces. *J. Phys.: Condens. Matter* **2012**, *24*, 064104.

(17) Bertrand, C. E.; Liu, K.-H.; Mamontov, E.; Chen, S.-H. Hydration-Dependent Dynamics of Deeply Cooled Water under Strong Confinement. *Phys. Rev. E* **2013**, *87*, 042312.

(18) Roh, J. H.; Briber, R. M.; Damjanovic, A.; Thirumalai, D.; Woodson, S. A.; Sokolov, A. P. Dynamics of tRNA at Different Levels of Hydration. *Biophys. J.* **2009**, *96*, 2755−2762.

(19) Wang, Z.; Fratini, E.; Li, M.; Le, P.; Mamontov, E.; Baglioni, P.; Chen, S.-H. Hydration-Dependent Dynamic Crossover Phenomenon in Protein Hydration Water. *Phys. Rev. E* **2014**, *90*, 042705.

(20) Meyer, A.; Dimeo, R. M.; Gehring, P. M.; Neumann, D. A. The High Flux Backscattering Spectrometer at the NIST Center for Neutron Research. *Rev. Sci. Instrum.* **2003**, *74*, 2759−2777.

(21) Mamontov, E.; Herwig, K. W. A Time-of-Flight Backscattering Spectrometer at the Spallation Neutron Source, BASIS. *Rev. Sci. Instrum.* **2011**, *82*, 085109.

(22) Inc., A. S. Discovery Studio Modeling Environment, 4.0; Accelrys Software Inc.: San Diego, CA, 2013.

(23) Dauberosguthorpe, P.; Roberts, V. A.; Osguthorpe, D. J.; Wolff, J.; Genest, M.; Hagler, A. T. Structure and Energetics of Ligand-Binding to Proteins - Escherichia-Coli Dihydrofolate Reductase Trimethoprim, a Drug-Receptor System. *Proteins: Struct., Funct., Genet.* **1988**, *4*, 31−47.

(24) Plimpton, S. Fast Parallel Algorithms for Short-Range Molecular-Dynamics. *J. Comput. Phys.* **1995**, *117*, 1−19.

(25) Lindner, B.; Smith, J. C. Sassena - X-ray and Neutron Scattering Calculated from Molecular Dynamics Trajectories using Massively Parallel Computers. *Comput. Phys. Commun.* **2012**, *183*, 1491−1501.

(26) Arnold, O.; Bilheux, J. C.; Borreguero, J. M.; Buts, A.; Campbell, S. I.; Chapon, L.; Doucet, M.; Draper, N.; Ferraz Leal, R.; Gigg, M. A.; Lynch, V. E.; Markvardsen, A.; Mikkelson, D. J.; Mikkelson, R. L.; Miller, R.; Palmen, K.; Parker, P.; Passos, G.; Perring, T. G.; Peterson, P. F.; Ren, S.; Reuter, M. A.; Savici, A. T.; Taylor, J. W.; Taylor, R. J.; Tolchenov, R.; Zhou, W.; Zikovsky, J. Mantid—Data Analysis and Visualization Package for Neutron Scattering and SR Experiments. *Nucl. Instrum. Methods Phys. Res., Sect. A* **2014**, *764*, 156−166.

(27) Roe, D. R.; Cheatham, T. E. PTRAJ and CPPTRAJ: Software for Processing and Analysis of Molecular Dynamics Trajectory Data. *J. Chem. Theory Comput.* **2013**, *9*, 3084−3095.

(28) Nguyen, H. Python front-end of cpptraj: a data analysis package for biomolecular simulation. https://github.com/Amber-MD/pytraj (accessed June 4, 2015).

(29) Doster, W.; Nakagawa, H.; Appavou, M. S. Scaling Analysis of Bio-Molecular Dynamics Derived from Elastic Incoherent Neutron Scattering Experiments. *J. Chem. Phys.* **2013**, *139*, 045105.

(30) Kawaguchi, T.; Kanaya, T.; Kaji, K. Fast Relaxations of Amorphous Polystyrene. *Phys. B* **1995**, *213-214*, 510−512.

(31) Kanaya, T.; Kawaguchi, T.; Kaji, K. Fast Process of Amorphous Polystyrene Below and Above the Glass transition Temperature T_g as Studied by Quasielastic Neutron Scattering. *J. Chem. Phys.* **1996**, *104*, 3841−3850.

(32) Arrese-Igor, S.; Arbe, A.; Frick, B.; Colmenero, J. Glassy Dynamics of Polystyrene by Quasielastic Neutron Scattering. *Macromolecules* **2011**, *44*, 3161−3168.

DOI: 10.1021/acs.jpcb.6b00866
J. Phys. Chem. B 2016, 120, 3232−3239

(33) Inoue, R.; Kanaya, T.; Nishida, K.; Tsukushi, I.; Shibata, K. Low-Energy Excitations and the Fast Process of Polystyrene Thin Supported Films Studied by Inelastic and Quasielastic Neutron Scattering. *Phys. Rev. E* **2006**, *74*, 021801.
(34) Bée, M. *Quasielastic Neutron Scattering*; Hilger: Bristol, England, 1988.
(35) Schiro, G.; Fichou, Y.; Gallat, F.-X.; Wood, K.; Gabel, F.; Moulin, M.; Hartlein, M.; Heyden, M.; Colletier, J.-P.; Orecchini, A.; Paciaroni, A.; Wuttke, J.; Tobias, D. J.; Weik, M. Translational Diffusion of Hydration Water Correlates with Functional Motions in Folded and Intrinsically Disordered Proteins. *Nat. Commun.* **2015**, *6*, 6490.
(36) Schiro, G.; Caronna, C.; Natali, F.; Cupane, A. Direct Evidence of the Amino Acid Side Chain and Backbone Contributions to Protein Anharmonicity. *J. Am. Chem. Soc.* **2010**, *132*, 1371−1376.

DOI: 10.1021/acs.jpcb.6b00866
J. Phys. Chem. B 2016, 120, 3232−3239